Metabolic pathways of *Plasmodium falciparum* as potent antimalarial drug targets

Short Summary of the Ph.D. thesis of

Richard Izrael

Supervisor: **Dr. Beáta G. Vértessy**

Institute of Molecular Life Sciences,

HUN-REN Research Centre for Natural Sciences,

Budapest, Hungary

Doctoral School of Multidisciplinary Medical Science,

Albert Szent-Györgyi Medical School

University of Szeged

Budapest

2024

List of publications that served as the basis of current Ph.D. thesis:

- **Izrael R**, Marton L, Nagy GN, Pálinkás HL, Kucsma N, Vértessy BG. Identification of a nuclear localization signal in the Plasmodium falciparum CTP: phosphocholine cytidylyltransferase enzyme. Sci Rep. 2020 Nov 12;10(1):19739. doi: 10.1038/s41598-020-76829-1. PMID: 33184408; PMCID: PMC7665022.
  IF: 4,38 / SJR Indicator: D1
- Babai R*, **Izrael R*,** Vértessy BG. Characterization of the dynamics of Plasmodium falciparum deoxynucleotide-triphosphate pool in a stage-specific manner. Sci Rep. 2022 Nov 19;12(1):19926. doi: 10.1038/s41598-022-23807-4. Erratum in: Sci Rep. 2023 Jan 3;13(1):102. PMID: 36402851; PMCID: PMC9675800. ***co-correspondence**
  IF: 4,6 / SJR Indicator: D1

List of publication not directly linked to current Ph.D. thesis:

- Guca E, Nagy GN, Hajdú F, Marton L, **Izrael R**, Hoh F, Yang Y, Vial H, Vértessy BG, Guichou JF, Cerdan R. Structural determinants of the catalytic mechanism of Plasmodium CCT, a key enzyme of malaria lipid biosynthesis. Sci Rep. 2018 Jul 25;8(1):11215. doi: 10.1038/s41598-018-29500-9. PMID: 30046154; PMCID: PMC6060094.
  IF: 4,011 / SJR Indicator: D1
- Molnár P, Marton L, **Izrael R**, Pálinkás HL, Vértessy BG. Uracil moieties in *Plasmodium falciparum* genomic DNA. FEBS Open Bio. 2018 Sep 29;8(11):1763-1772. doi: 10.1002/2211-5463.12458. PMID: 30410856; PMCID: PMC6212640.
  IF: 1,959 / SJR Indicator: Q2
- Molnár P, Orbán Á, **Izrael R,** Babai R, Marton L, Butykai Á, Karl S, Vértessy BG, Kézsmárki I. Rapid and quantitative antimalarial drug efficacy testing via the magneto-optical detection of hemozoin. Sci Rep. 2020 Aug 20;10(1):14025. doi: 10.1038/s41598-020-70860-y. PMID: 32820190; PMCID: PMC7441145.
  IF: 4,38 / SJR Indicator: D1

INTRODUCTION

After decades of international effort for its eradication, malaria is still considered one of the most impactful vector-borne disease, affecting approximately 250 million people each year and leading to around 650,000 deaths just in 2022, out of which 80% were children under the age of 5[1]. The disease is caused by the protist *Apicomplexan* parasite of the *Plasmodium* genus, most notably *Plasmodium falciparum*, which is responsible for most lethal infections in the Sub-Saharan Africa. Due to increased prevalence of resistant parasites to the primary line of defence artemisinin derivatives[2], urgent development of novel antimalarial drugs and the identification of potent drug targets are needed.

Malaria parasites exhibit a complex multi-host life cycle that consists of two stages: a sexual life cycle in the mosquito vector and an asexual life cycle in the human host. The asexual life cycle is responsible for the symptomatic malaria, hence it is the main target of drug development. During the mosquito bite, sporozoites are injected from the midgut of the mosquito into the sub-cutaneous capillaries and they travel to the liver through the blood stream, where parasites enter the hepatocytes. After a short 1-week long incubation period, parasites egress as merozoites and enter the intraerythrocytic life cycle upon infecting red blood cells (RBCs) (Figure 1.).

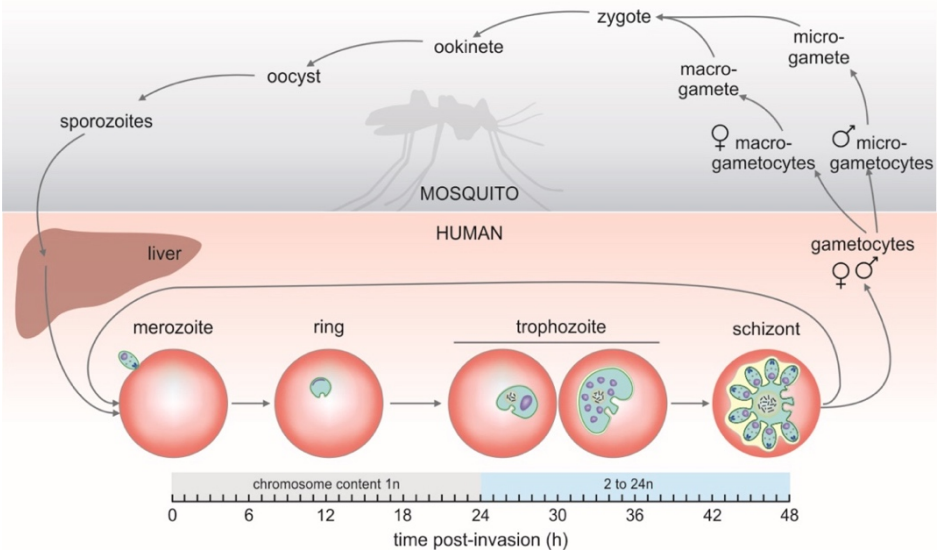

Figure 1. The complex life cycle of Plasmodium parasites[37].

The intraerythrocytic starts with the formation of ring stage parasites, named after its peculiar morphology. This phase is analogous to the G1 of the cell cycle, where parasites accumulate the necessary nutrients for the subsequent DNA replication[3,4]. The primary source

of metabolites is hemoglobin, which is found in abundance within the RBCs. After 24 hours, ring parasites develop into trophozoites, when the majority of DNA replication occurs. During this short 16-hour time period, the parasite's genome is replicated into up to 32 copies. Finally, the last 8 hours of the 48-hour intraerythrocytic life cycle is the schizont stage, when the newly formed daughter merozoites are segmented, and the egress of parasites begin the next cycle.

The formation of several daughter cells within a 48-hour time frame puts immense metabolic pressure on the parasite, requiring the biosynthesis of several biomolecules. Out of major importance, phospholipid membranes[5–7] and nucleic acids[8–10] are amongst the most required biomolecules that needed to be synthesized during the intraerythrocytic life cycle, hence indicating their potential as antimalarial drug targets[11]. In my thesis, I am focusing on characterizing certain aspects of the phospholipid (PL) and nucleotide metabolism. This research aims to provide further support for utilizing the highlighted pathways in the development of innovative antimalarial drugs and gaining useful insights into their mechanism of action

During the intraerythrocytic life cycle, the parasite relies heavily on phospholipid biogenesis to support the immense need for new membrane structures in the fast-proliferating parasite. The major contributor of PL membranes is phosphatidylcholine (PC), which provides 45-55% of the total PL content[6]. Upon invasion, the total lipid content of infected RBC increases from 35% PL to 60%, further highlighting the abundance of membrane generated in only 48 hours. As RBCs do not synthesize lipids, the parasite has to generate PLs *via de novo* biosynthesis, which has been shown to be essential in blood stages[12,13], further proving its potential as an antimalarial drug target. A choline analogue lead compound, albitiazolium has already been evaluated in human phase II clinical trial but has been discarded due to poor pharmacokinetic properties[14].

The PL metabolic pathway or as often referred to as, the Kennedy pathway is an intertwined set of parallel metabolic routes, which allows the turnover of one PL species to another (Figure 2.)[15]. Focusing on the most abundant PL, PC can be generated *via* several metabolic routes. The primary source of choline comes from the exogenous source of lyso-phosphatidylcholine (LysoPC) or in the form of choline (Cho). The choline is then turned into phosphocholine (P-Cho) by the choline kinase (CK) enzyme. The second and rate-limiting step is catalysed by the CTP:phosphocholine cytidylyltransferase (CCT) enzyme, which turns P-Cho into CDP-choline (CDP-Cho) by conjugating a cytidine-diphosphate (CDP) and leaving a pyrophosphate as a by-product. The CCT enzymes is crucial in the regulation of PC

biosynthesis, therefore considered a highly potent antimalarial drug target and the main focus of the current thesis. Finally, CDP-Cho is used to generate PC by attaching the phosphobase onto a diacyl-glycerol (DAG), which step is catalysed by the membrane-associated protein choline-ethanolamine phosphotransferase (CEPT).

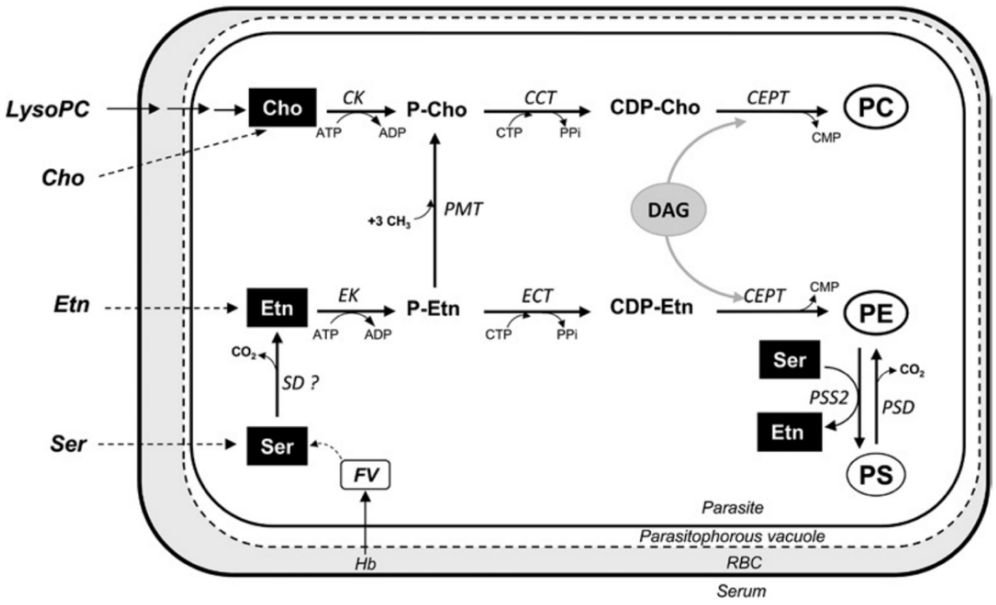

Figure 2. Phospholipid metabolism of Plasmodium falciparum.[15]

The *Pf*CCT protein catalyses the rate-limiting step of the PC biosynthesis in the malaria parasite, therefore its crucial to investigate structural and sequential differences in the enzyme. While most eukaryotic CCTs are homodimers, *Pf*CCT is a pseudo-heterodimer protein due to a gene duplication event that resulted in the two monomers to be on a single polypeptide chain. The monomers consist of a catalytic domain and the regulatory M domain, while there is a 200 amino acid-long inter-linker domain between the two repeat unit that has not yet been associated with any further function. A major structural difference is the lack of N-terminal nuclear localization signal (NLS) coding element and the C-terminal phosphorylation site, neither of which has been identified in *Pf*CCT.

The regulation of the protein occurs *via* a mechanism noted as translocation. In the inactive state, the CCT enzyme is in soluble form, where the autoinhibitory helix (AI) in the M domain is bound to the αE helix of the C domain, rendering it catalytically suppressed[16,17]. Upon low PC content of membrane surface, the physicochemical properties of membranes change. Low PC content leads to increased membrane curvature due to the accumulation of negatively charged PLs, which also changes the surface charge and gives rise to membrane packing defects[18–20]. CCT enzyme can sense these changes in the membrane properties, eliciting conformational changes in the M domain and allowing the embedding of the membrane-

induced amphipathic helix (m-AH), while lifting the inhibition of the catalytic domain[19,20]. There are key differences in the putative structure and localization of the *Pf*CCT protein, most notably in the m-AH domain, which instead of a long continuous helix it is split into two, a shorter m-AH-N and a longer m-AH-C helices[21]. This indicates a slightly different molecular dynamic of the translocation, which would explain the mere 6-fold increase in activity increase upon translocation, compared to the more than 100-fold difference in mammalian CCTs[22]. Furthermore, the predominant CCT isoform in eukaryotic cells is the nuclear CCTα/CCT1, which has been shown to be able to translocate to the cytosol upon increased demand for PC biosynthesis. In *P. falciparum*, *Pf*CCT is localized diffusely in late-stage parasites and has not been characterized for its translocation capabilities in a cellular environment[23].

Previously, a Chinese Hamster Ovary (CHO) based thermosensitive CCT mutant cell line called CHO-MT58 has been generated *via* chemical mutagenesis[24–26] and has been shown previously to be a good system for heterologous characterization of orthologue CCT proteins, including *Pf*CCT[27]. Due to a point mutation in the endogenous CCT, increasing the incubation temperature from 37°C to 40°C leads to 90% drop in choline content after 24 hours and apoptosis after 48 hours[28], providing a useful tol to characterize CCT proteins in a cellular environment without the need for transgenic disruption of the endogenous CCT.

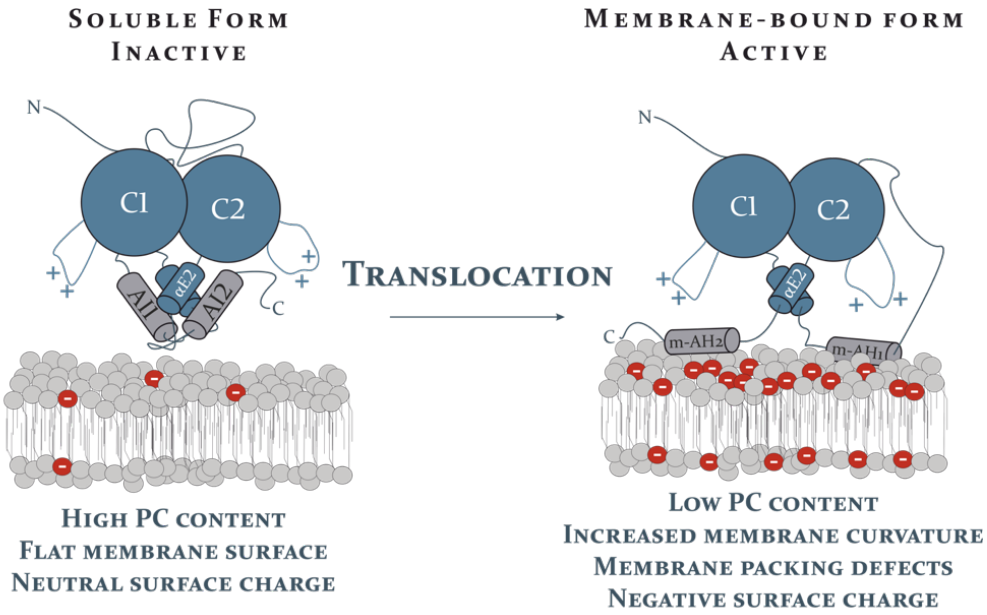

Figure 3. Putative translocation mechanism of PfCCT. *In the inactive state, the catalytic domains (C1 and C2, blue) PfCCT is inhibited by the autoinhibitory helix (AI) in its membrane-binding domains (M, grey). Upon decreased PC content in the membrane, the catalytic domain is released from its inhibition and conformational changes are induced to turn into a membrane-induced amphipathic helix (m-AH).*

Nucleotide metabolism is another proven metabolic pathway to be targeted for antimalarial drug development. Nucleic acid biosynthesis is crucial for the fast proliferation of parasites during the intraerythrocytic life cycle for both DNA replication and RNA polymerization[29,30], hence the generation of large quantities of their building blocks, deoxyribonucleotide triphosphates (dNTP) and ribonucleotide triphosphates (NTP) respectively, are essential for its survival. The purine and pyrimidine nucleotide metabolism of the malaria parasite is essentially different, as purine biosynthesis relies on salvaging the nucleobases and nucleosides from the blood stream, while pyrimidine biosynthesis occurs solely *via de novo* biosynthesis. Therefore, the pyrimidine metabolic pathway has been long considered a potent antimalarial drug target, with several already existing compounds targeting the crucial thymidylate synthase-dihydrofolate reductase (TS-DHFR) enzyme [30].

Purine metabolism precursors are derived from the blood stream of the human host, most notably adenozin, hypoxanthine and xanthine. However, adenosine is used extensively by red blood cells to generate energy by phosphorylating it into ATP. Phosphorylated nucleotides cannot be imported into the parasite due to the lack of transporters, which allow only the import of nucleosides or the nucleobases. Generally, nucleosides are first turned into their respective nucleobases, which is then conjugated with a phosphoribosyl-group to be turned into ribonucleotide and subsequently, deoxyribonucleotide phosphates. The oxidation is catalysed by the ribonucleotide reductase (RNR) enzyme complex, that turns the nucleotide diphosphate (NDP) form into the respective deoxyribonucleotide diphosphate (dNDP) for both pyrimidine and purine nucleotides.

Pyrimidine metabolism requires the generation of several, energetically expensive molecules as there is no reported way to transport pyrimidine precursors into the parasite. The pathway is very similar in nature to the human host's, although the catalysing enzymes have unique characteristics and key differences in comparison, providing several targets for drug development.

Interestingly, the dNTP pool of the parasite has not yet been characterized extensively neither throughout the intraerythrocytic life cycle, nor under drug pressure. Here, I wish to investigate how it is impacted by the addition of a pyrimidine metabolic drug and how it may contribute to the rapid emergence of drug resistance in the field.

AIMS

In the present PhD thesis, I focus on several aspects of two crucial metabolic pathways of the malaria parasite, *Plasmodium falciparum*. The phospholipid biosynthesis and nucleotide metabolism are both crucial processes in the fast-proliferating intraerythrocytic life cycle of the malaria parasite, therefore they are ideal candidates for future drug development and their elaboration is of outmost importance for the identification of novel drug targets.

First, I wished to characterize the major structural differences of the rate-limiting phosphatidylcholine biosynthetic enzyme, CTP:phosphocholine cytidylyltransferase. For that, I investigated the key characteristics of the *Pf*CCT protein, where I identified a putative nuclear localization signal in the lysine-rich insertion. Furthermore, I wished to exploit the CHO-MT58 cellular model to dissect the functional role of *Plasmodium*-specific regions of the *Pf*CCT protein and their impact on cellular localization. I also investigated the rescue potential of several truncated *Pf*CCT constructs based on the first and second monomer of the pseudo-heterodimer enzyme by transiently transfecting the CHO-MT58.

Second, I investigated the temporal dynamics of the expression of purine and pyrimidine metabolic enzymes during the intraerythrocytic life stages using high-quality transcriptomic data from databases. In tandem, I wanted to quantify the level of each dNTP across the ring, trophozoite and schizont stages of the parasite. Finally, I wished to characterize the impact of pyrimidine metabolic drugs on the level of dNTPs upon drug exposure at different concentrations. For that, I have chosen a potent TS-DHFR inhibitor called WR99210, which has been previously shown to have a sub-nanomolar effective concentration on blood stage parasites[91]. The goal of these findings is to understand how antimalarial drug resistance occurs so rapidly in parasites under drug exposure and imbalances in the nucleotide homeostasis can lead to valuable answers regarding this matter.

MATERIALS AND METHODS

Firstly, for the characterization of the *Pf*CCT, I focused on *in silico* investigation of the *Plasmodium*-specific structural elements. I used ClustalOmega to generate multiple sequence alignment and used SwissModel for homology modelling of the *Pf*CCT catalytic domain with the lysine-rich insert based on the currently available *Pf*CCT crystal structure (PDB: 4ZCS)[32]. Nuclear localization signal prediction has been carried using *cNLSmapper* tool with default settings.

The role of the identified unique structural elements has been characterized using the thermolabile CCT mutant CHO-MT58 cell line with both immunofluorescence-based colocalization analysis and flow cytometry-based rescue assay. CHO-MT58 cells were transfected with M domain or lysine-rich insertion (ΔK) truncated constructs (Figure 3.). Colocalization analysis has been carried out using Zeiss LSM 710 Confocal Microscope and 8-bit images were analysed using *FiJi* Coloc 2 plugin. Nuclear overlap coefficient was determined based on the Mander's correlation formula: $M = \frac{\sum_i S1_{i,coloc}}{\sum_i S1_i}$, where $S1_{i,coloc}$ equals $S1_i$, the intensity of the CCT signal of each pixel where the nuclear DAPI signal is above the determined threshold.

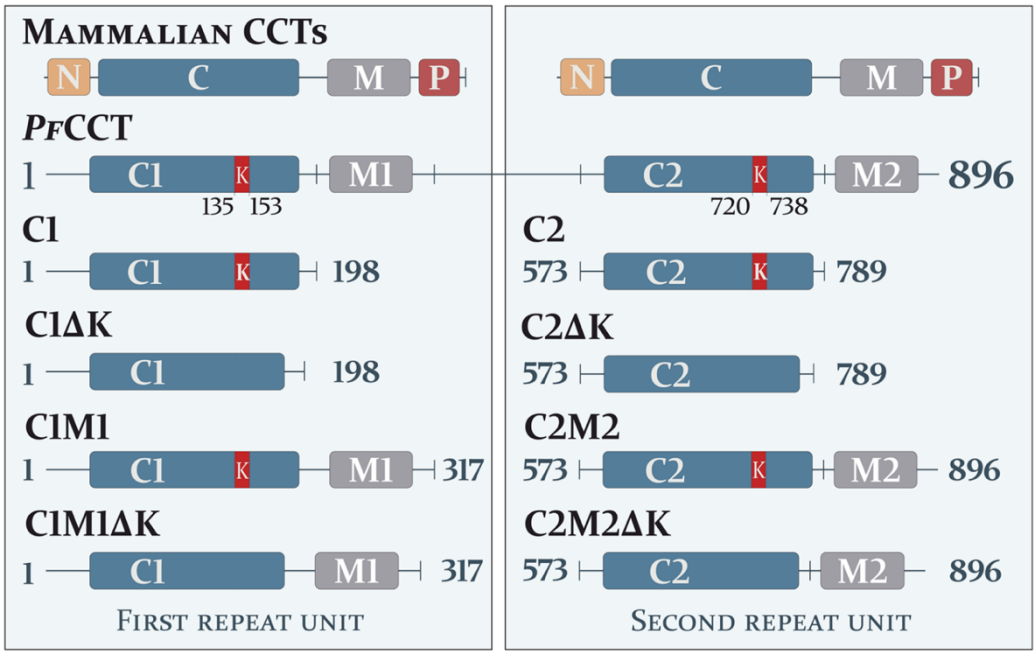

Figure 3. Schematic representation of the investigated PfCCT constructs. *C (blue) and M (grey) refers to the catalytic and membrane-binding domain of the first and second catalytic domain, respectively. ΔK indicates the deletion of the lysine-rich loop shown in red box. P (red) and N (orange) indicates the N-terminal NLS and the phosphorylation domain of mammalian CCTs.*

To check the rescue potential of the constructs, transiently transfected CHO-MT58 cells have been incubated for 3 days at the permissive 37°C and restrictive 40°C temperature, then 1 µg/ml of propidium-iodide (PI) has been added to stain dead cells in the complete culture. Transfection efficiency was considered by gating to enhanced green fluorescent protein (EGFP) signal, which was encoded on the transfected plasmid and expressed independently of each construct by including an internal ribosome entry site (IRES) upstream of the *egfp* gene on the plasmid. The rescue potential has been calculated using the following mathematical formula:

$$Rescue\ potential\ (\%) = \frac{\frac{All\ cells - PI^{+}\ cells}{All\ cells}\ at\ 40°C}{\frac{All\ cells - PI^{+}\ cells}{All\ cells}\ at\ 37°C} * 100$$

Secondly, transcriptomic data analysis of nucleotide metabolic enzymes has been carried out using a high-quality transcriptomic dataset from the PlasmoDB database (*plasmodb.org*), where RNA-Seq transcriptomic data generated by Toenhake *et al.*[33] is publically available. Values are determined in fragments per kilobase exon per million of mapped reads (FPKM) to quantify RNA expression levels.

Complete dNTP pool was isolated from double sorbitol synchronised *P. falciparum 3D7* parasites for ring (6-12 hours post invasion), trophozoite (30-36 hours post invasion) and schizont (42-48 hours post invasion). For each stage, 300 µl of pellet was collected. WR99210-treated samples were split into 3 from the same starting culture following the second sorbitol synchronization. WR99210 has been added immediately after in two concentrations (1 nM and 10 nM), diluted in complete malaria culture medium and dNTP was isolated 24 hours after drug addition, corresponding to the trophozoite stage sample.

dNTP isolates were measured with a novel EvaGreen-based fluorescent nucleotide quantification method developed by *Purhonen et al.*[34]. The method uses a 197-nucleotide long synthetic oligonucleotide template that starts with a short primer-binding site directly adjacent to a single dNTP detection site, followed by a long stretch of other bases to amplify the signal coming from the double stranded DNA dye, EvaGreen. The main principle of the assay is that each template contains only one complementary base of the determined dNTP, which limits the polymerization during the amplification. Consequently, the more of the quantified dNTP was in the sample initially, the more product there will be, hence higher fluorescence signal.

RESULTS

In silico investigation of *Pf*CCT specific structural elements revealed crucial differences in comparison with mammalian CCTs from rat (*Rattus norvegicus – Rn)* and human (*Homo sapiens – Hs*). It has been previously demonstrated the catalytic domain is highly conserved across orthologues, with a major difference (Figure 4.). *Pf*CCT contains an 18-amino acid long, lysine-rich insertion, which is a very specific trait possessed across the species of the *Apicomplexa* genus.

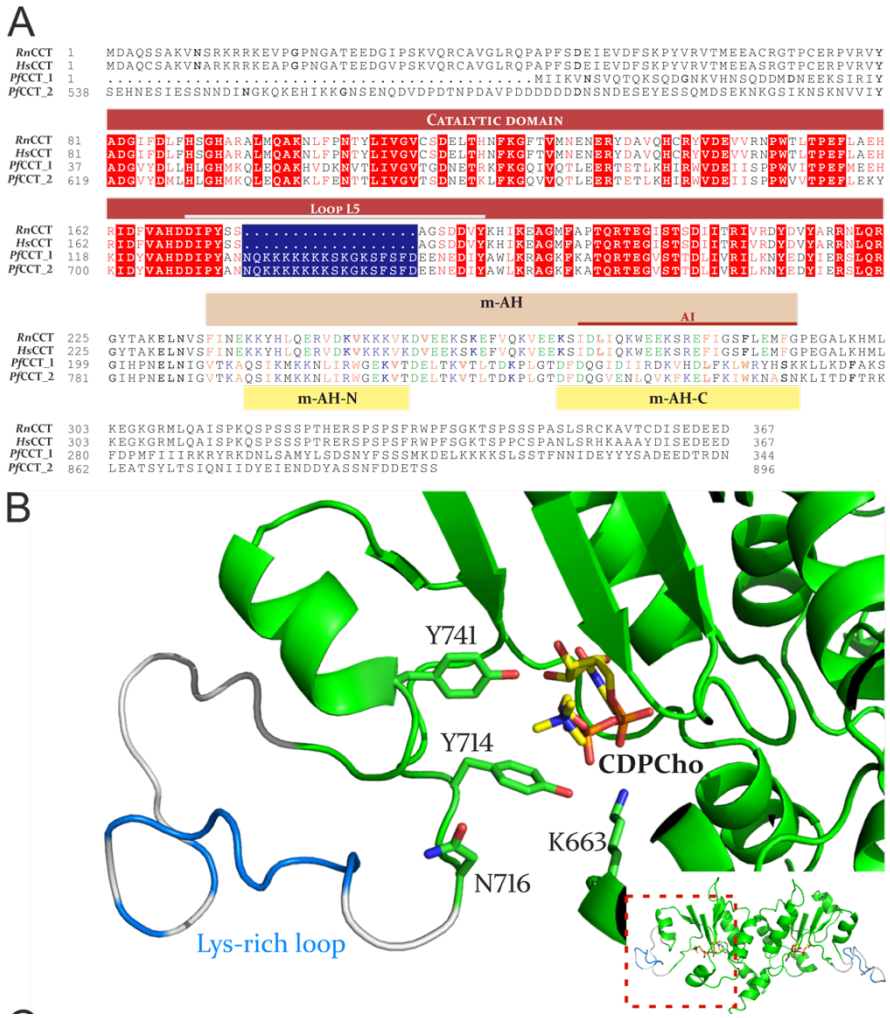

Figure 4. A) Multiple sequence alignment of rat, human and Plasmodium falciparum CCT proteins. B) Homology model of PfCCT lysine-rich insertion. The lysine-rich insertion is a flexible loop region, therefore the model only shows a representative conformational state.

The Lys-rich insertion has been previously demonstrated to be dispensable as its deletion did not impact the catalytic activity of a catalytic domain construct of *Pf*CCT[35]. However, its role has not been characterized in the presence of the M domain or *in vivo*, which begs the question how the Lys-rich insertion influences the regulation of *Pf*CCT. Based on the positioning of this insertion, it is found on a solvent accessible surface and according to the

low QMEAN local quality score, it has a flexible nature, which argues for its role in interaction with other molecules or the M domain. NLS prediction revealed that the region might serve as a weak bipartite NLS with a score of 5.8. Furthermore, the M domain has also shown to contain two predicted NLS motifs.

To verify their NLS function, I carried out immunofluorescence-based colocalization analysis (Figure 5). The truncation of both the M domain and/or the lysine-rich insertion (ΔK) lead to a decreased propensity of nuclear fluorescence signal. I also investigated the translocation capabilities *via* phospholipase C treatment, which excises PC in membranes and leads to PC depleted state, triggering CCT translocation in the process. In case of the full length *Pf*CCT and second repeat unit C2M2 construct the translocation has occurred, proving its potential to translocate.

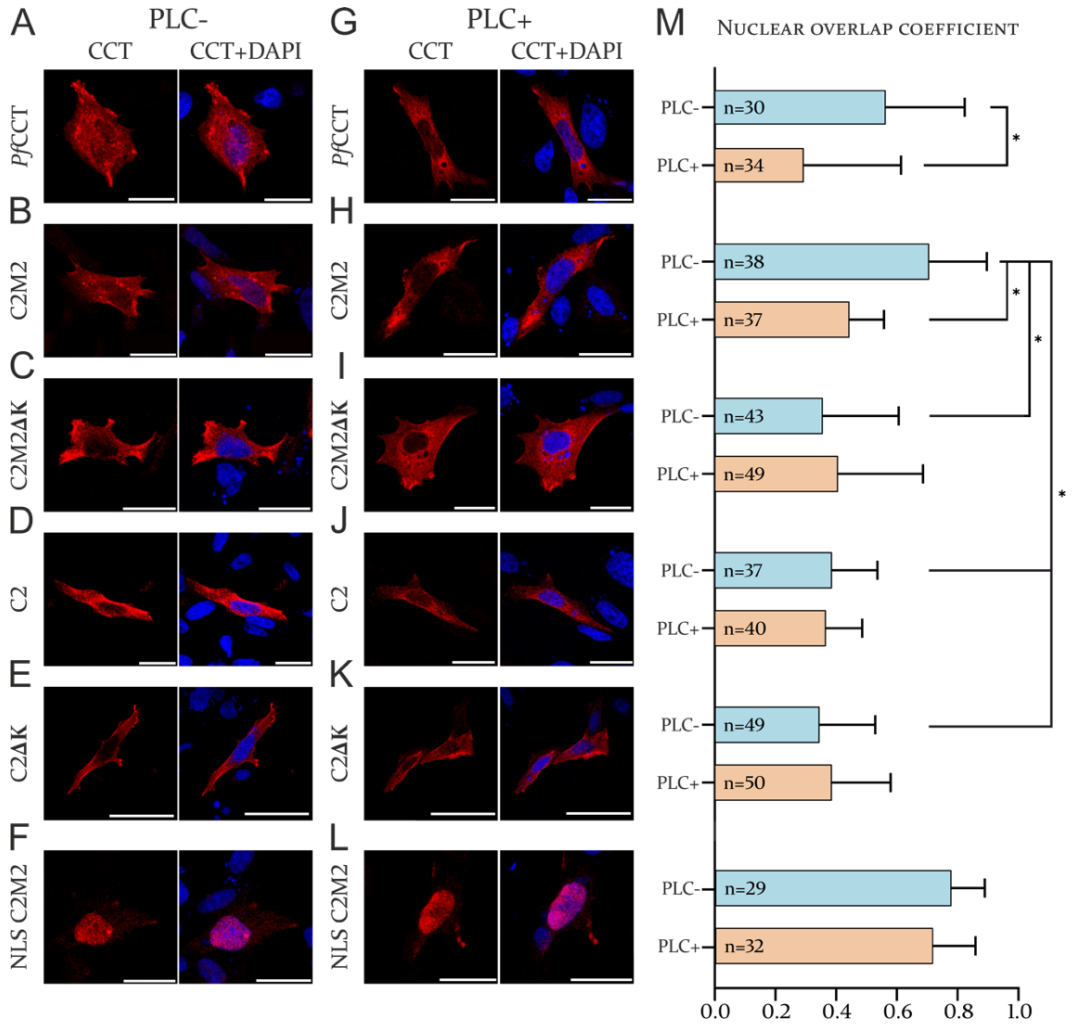

Figure 5. Colocalization analysis of the different PfCCT constructs in CHO-MT58 cells. *Confocal microscopy images of the full length PfCCT (A), second repeat unit C2M2 (B), the Lys-rich loop deleted C2M2ΔK (C), the M domain truncated C2 (D), the double truncated C2ΔK (E) and SV40 NLS-tagged C2M2 constructs (F) and the respective PLC treated samples (G-L). Nuclear overlap coefficient was calculated using Fiji (*p < 0.001). The number in the bar indicates the number of cells considered for the statistical analysis.*

The *in vivo* impact of the truncation of *Pf*CCT was investigated by transiently transfecting the different *Pf*CCT constructs into the CCT-mutant CHO-MT58 cell line. Rescue potential was then determined by flow cytometry analysis based on the quotient of living cells grown at the permissive 37°C and restrictive 40°C temperatures, respectively. The assay revealed that the lysine-rich insertion is not essential for the *in vivo* rescue of the CHO-MT58 cells in either repeat units of *Pf*CCT (Figure 6.). Additionally, the M domain was also shown to be dispensable for the *in vivo* activity, which has been suggested based on the constitutive activity of M domain truncated constructs *in vitro.* Here, I also demonstrated the use of *Hs*CCT in the CHO-MT58 cell line and its potential to rescue CHO-MT58 cells.

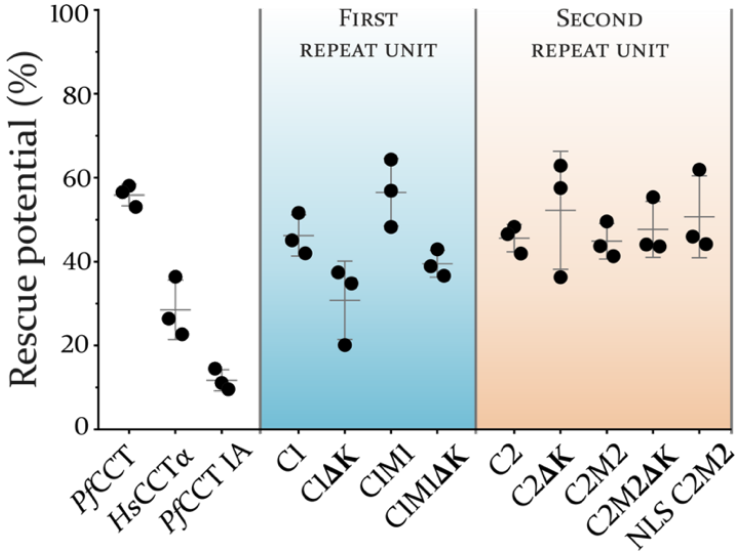

Figure 6. Rescue potential of the different PfCCT constructs in the thermosensitive CCT-mutant CHO-MT58 cell line. *All experiments were carried out in triplicates, results are shown as average±S.D.*

The pyrimidine biosynthetic pathway starts with the generation carbamoyl-phosphate, catalysed by the carbamoyl-phosphate synthase II enzyme, which is one of the most abundant transcript of all enzymes (Figure 7). The pathway is then continued linearly until the synthesis of UMP, the common precursor of both deoxycytidine-triphosphate (dCTP) and thymidine-triphosphate (dTTP). The path then branches out to generate either nucleotide. Based on the transcriptomic analysis of pyrimidine nucleotide metabolic enzymes, it revealed that the enzymes that lead up to UMP show a slightly different transcriptomic profile compared to the later enzymes of the pathway. A 5-hour shift in peak expression is present from early (30 hours post invasion peak) to late (35 hours post invasion peak) enzymes. Additionally, early enzymes start expressing in low amounts in ring stages, while the transcript of the late enzymes is absent at this stage.

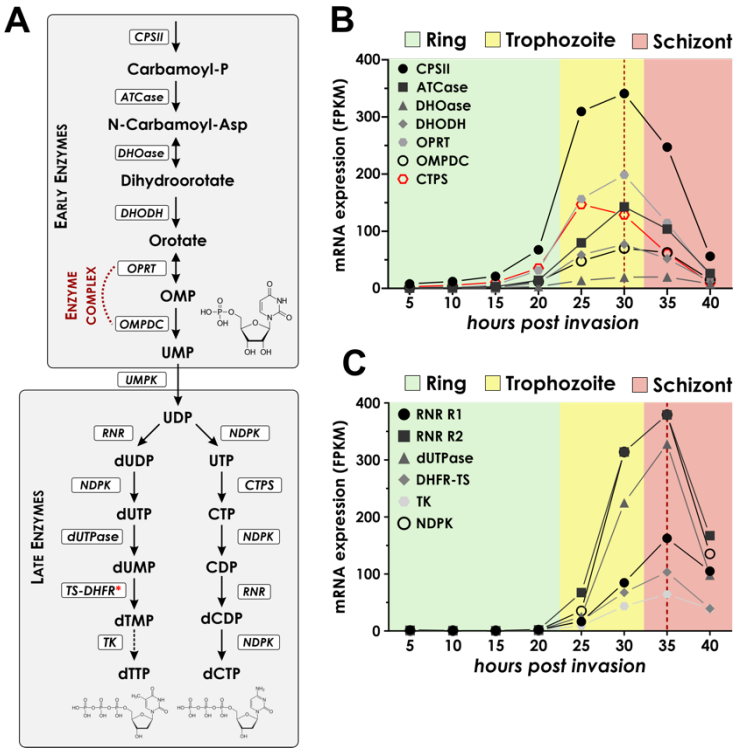

Figure 8. Transcriptomic analysis of pyrimidine metabolic enzymes. *A) Pyrimidine metabolic pathway of Plasmodium falciparum. Transcriptomic profile of early (B) and late (C) pyrimidine biosynthetic enzymes. CPSII – carbamoyl-phosphate synthase II, ATCase – aspartate transcarbamoylase, DHOase – dihydroorotase, DHODH – dihydroorotate dehydrogenase, OPRT - orotate phosphoribosyl transferase, OMPDC – OMP decarboxylase, RNR – ribonucleotide reductase, NDPK – nucleotide diphosphate kinase, CTPS – CTP synthase, TS-DHFR – thymidylate synthase-dihydrofolate reductase, TK – thymidylate kinase*

Purine nucleotide biosynthetic enzymes showed a similar trend to that of early pyrimidine nucleotide metabolic enzymes, with a peak expression at 30 hours post invasion and detectable level of transcripts during the ring stage. Amongst all enzymes, the broad substrate specific hypoxanthine-guanine-xanthine phosphoribosyl transferase shows the highest expression, the

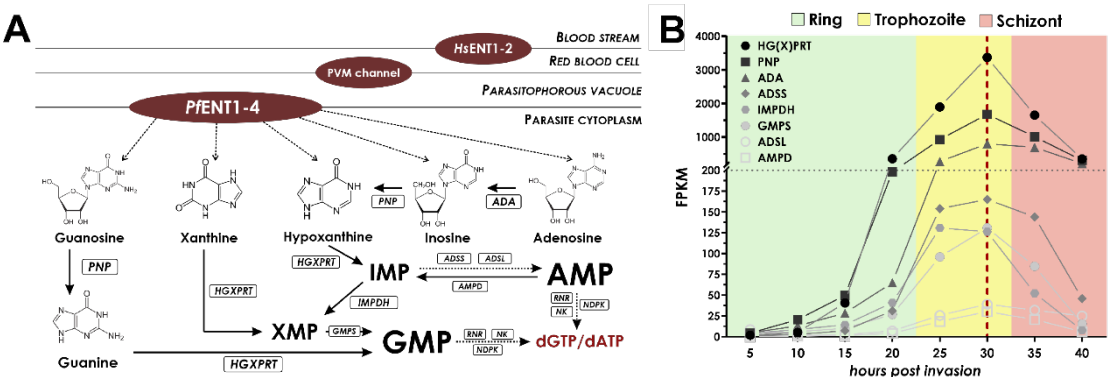

Figure 7. Transcriptomic analysis of purine metabolic enzymes*. A) Purine metabolic pathway of Plasmodium falciparum. B) Transcriptomic profile of purine biosynthetic enzymes.*
ENT – equilibrative nucleoside transporter, PVM – parasitophorous vacuole membrane,
ADA – adenosine deaminase, ADSL – adenylosuccinate lyase, ADSS – adenylosuccinate synthase,
AMPD – AMP deaminase, GMPS – GMP synthase, HGXPRT – hypoxanthine-guanine-xanthine phosphoribosyl transferase, IMPDH – IMP dehydrogenase, NK – nucleoside kinase,
NDPK – nucleoside diphosphate kinase, PNP – purine nucleoside phosphorylase

gateway to all purine nucleotides. Furthermore, RNR, another enzyme with an even broader substrate range has shown to be expressed abundantly, indicating the excess need for these enzymes and their potential as antimalarial drug targets.

Investigation of dNTP levels across the intraerythrocytic stages shows the accumulation of dNTPs starting in ring stages. Ring samples contain approximately 18 fmol per million parasites. In this stage, the most abundant dNTP is dATP with approximately 54.4% ± 8.9% of the total dNTP amount. It is closely followed by similar levels of dTTP and dCTP corresponding to around 23.1% ± 10.6% and 19.1% ± 1.9% of the total dNTP amount, respectively. dGTP showed the lowest amount with levels barely above the limit of quantification, representing only 3.4% ± 2.9% of the total dNTP pool. As expected, based on the transcriptomic analysis, dNTP levels significantly increase by the trophozoite stage by 10-fold with an overall ca. 180 fmol total dNTP in million parasites. There is also an observable shift in the dNTP composition of this stage. Instead of dATP, dTTP is the most abundant with 40.1% ± 6.5% relative dNTP amount, then dATP and dCTP represents approximately the same ratio with 21.4% ± 1.3% and 30.1% ± 3.2%, respectively. dGTP is still the least represented dNTP with only 8.4% ± 7.4% of the total dNTP pool. Finally, the schizont stage parasites displayed a very similar overall distribution in terms of their dNTP composition in comparison to trophozoite stage parasites, although the total dNTP slightly decreased with ca. 140 fmol total dNTP per million parasites. The relative proportion of dTTP is still the highest with 43.5% ± 6.2%, then dATP and dCTP accounts for 17.8% ± 3.8% and 32.8% ± 0.4%, respectively. As seen previously, dGTP represents the least portion of the dNTP pool, representing only 6.0% ± 3.7% of the total dNTP levels.

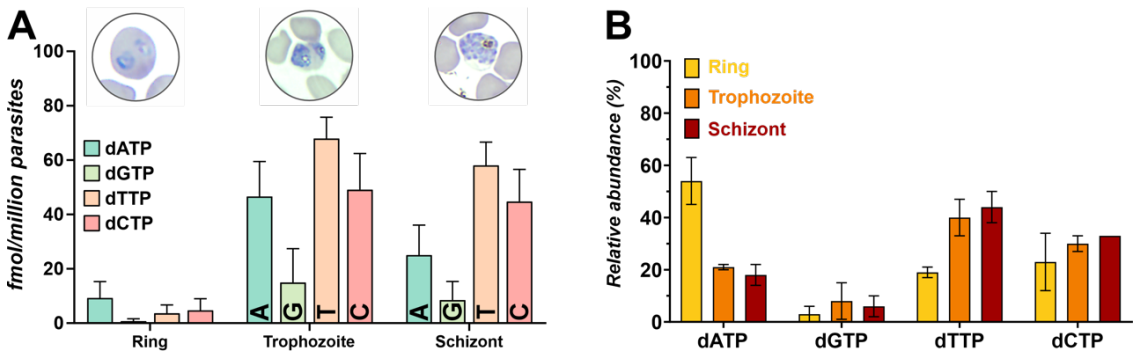

Figure 9. dNTP levels across the stages of the intraerythrocytic life cycle.
Absolute (A) and relative (B) levels are shown as average ± S.E.M. of triplicates.

To investigate the impact of pyrimidine metabolic drugs, WR99210 has been added to the cultures in 1 nM and 10 nM concentrations to double sorbitol synchronised rings and treated

for 24 hours. Interestingly, in case of the 1 nM WR99210 treatment, no difference was observed compared to the non-treated sample after 24 hours. It has been previously established that WR99210 starts to be effective in late-stage parasites in a stage-specific manner[36]. However, in the 10 nM WR99210 treated samples a very prominent effect was observed. As expected, dTTP levels diminished completely and showed levels below the limit of quantification (Figure 10.). While dCTP and dATP levels were not affected, dGTP levels also diminished, a surprising result that has not yet been observed.

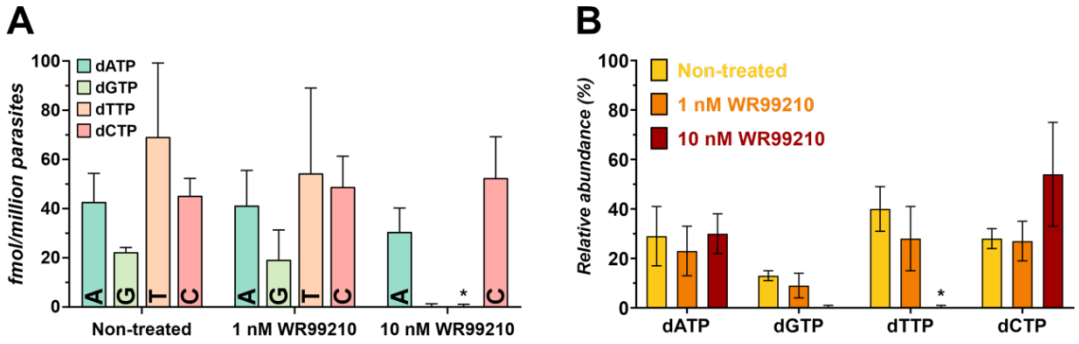

Figure 10. dNTP levels under WR99210 drug pressure.
Absolute (A) and relative (B) dNTP amount is represented by average ± S.E.M. values.

SUMMARY

In summary, my *in silico* investigation of *Plasmodium*-specific structural elements revealed two potential motifs that could contribute to cellular localization. My findings in the CCT-mutant CHO-MT58 cell line showed that both the lysine-rich insertion and/or the M domain is required for nuclear localization. Furthermore, I showed that the *Pf*CCT enzyme is capable of relocation upon phospholipase C-induced PC depletion. Finally, rescue assay showed that neither of these structural elements are essential for *in vivo* rescue of the CHO-MT58 cell line, showing a more robust catalytic efficiency of the *Pf*CCT enzyme.

On the other hand, nucleotide metabolism has been dissected and characterized in detail to elucidate the temporal dynamics of the purine and pyrimidine biosynthetic pathways. Transcriptomic analysis revealed an interesting shift in peak expression from early to late metabolic enzymes of the pyrimidine metabolic enzymes. Moreover, enzymes with a broad substrate specificity show the highest expression in good correspondence with their excess need. dNTP levels across the intraerythrocytic stages demonstrate that trophozoites are the most abundant in total dNTP. dNTP composition shifts from ring to trophozoite stage, where instead of dATP, dTTP becomes the most abundant. Treatment of WR99210 had an unexpected impact on cellular dGTP levels, as well as diminished dTTP levels, which could indicate how a perturbed nucleotide pool could contribute to antimalarial drug resistance.

THESES POINTS OF MY PHD THESIS

The theses points of the current PhD are as follows:

Phospholipid metabolism

- I characterized the full length *Pf*CCT *in silico* and identified the lysine-rich insertion and the M domain as modulators of subcellular localization. I hypothesized their role in the translocation mechanism of the *Pf*CCT enzyme and how this unique element of *Apicomplexan* CCT proteins might indicate a structurally different regulation of the enzyme.
- I proved the role of the Lys-rich loop and the M domain in the nuclear localization of the protein using confocal microscopy-based colocalization analysis. I also demonstrated the translocation capabilities of the full length *Pf*CCT enzyme and the second repeat unit construct by inducing PC depleted membranes using PLC.
- I investigated the role of the unique *Plasmodium*-specific structural elements in their impact on *in vivo* rescue potential of the thermosensitive CCT-mutant CHO-MT58 cell line. I demonstrated that both the Lys-rich insertion and the M domain is dispensable to rescue the cells at the restrictive 40°C temperature. I also showed that the *Hs*CCTα is capable of rescuing the cells, further proving the concept of a cellular model for *Pf*CCT specific drug development.

Nucleotide metabolism

- I gathered high-quality RNA-Seq transcriptomic data about the pyrimidine and purine nucleotide metabolic enzymes and dissected their temporal dynamics throughout the intraerythrocytic life cycle of the *Plasmodium falciparum* parasite. It revealed differences in expression of the early and late pyrimidine metabolic enyzmes.
- I measured the level of the canonical dNTPs across the major intraerythrocytic ring, trophozoite and schizont life cycle stages, where I found that total dNTP is relatively low in ring stages and reaches its maximum at the trophozoite stage. dTTP was found to be the most abundant dNTP, followed by dATP and dCTP with similar levels and dGTP represented the lowest amount across all stages.
- I observed that the TS-DHFR inhibitor, WR99210 had a significant impact on both dTTP and surprisingly, dGTP levels in the 10 nM concentration after 24 hours of treatment.

REFERENCES

1. World Health Organization. *World Malaria Report 2023*. https://www.who.int/publications/i/item/9789240086173 (2023).
2. Ward, K. E., Fidock, D. A. & Bridgford, J. L. Plasmodium falciparum resistance to artemisinin-based combination therapies. *Curr Opin Microbiol* **69**, 102193 (2022).
3. Lee, A. H., Symington, L. S. & Fidock, D. A. DNA Repair Mechanisms and Their Biological Roles in the Malaria Parasite Plasmodium falciparum. *Microbiology and Molecular Biology Reviews* **78**, 469–486 (2014).
4. Matthews, H., Duffy, C. W. & Merrick, C. J. Checks and balances? DNA replication and the cell cycle in Plasmodium. *Parasit Vectors* **11**, 1–13 (2018).
5. Wengelnik, K. *et al.* A Class of Potent Antimalarials and Their Specific Accumulation in Infected Erythrocytes. *Science (1979)* **295**, 1311–1314 (2002).
6. Gulati, S. *et al.* Profiling the Essential Nature of Lipid Metabolism in Asexual Blood and Gametocyte Stages of Plasmodium falciparum. *Cell Host Microbe* **18**, 371–381 (2015).
7. Vial, H. J., Eldin, P., Tielens, A. G. M. & van Hellemond, J. J. Phospholipids in parasitic protozoa. *Mol Biochem Parasitol* **126**, 143–154 (2003).
8. María Belén Cassera. Purine and Pyrimidine Pathways as Targets in Plasmodium falciparum. *Current Topics in Medincinal Chemistry* **23**, 1–7 (2011).
9. Frame, I. J., Deniskin, R., Arora, A. & Akabas, M. H. Purine import into malaria parasites as a target for antimalarial drug development. *Ann N Y Acad Sci* **1342**, 19–28 (2015).
10. Krungkrai, S. R. & Krungkrai, J. Insights into the pyrimidine biosynthetic pathway of human malaria parasite Plasmodium falciparum as chemotherapeutic target. *Asian Pac J Trop Med* **9**, 525–534 (2016).
11. Alam, A. *et al.* Novel antimalarial drug targets: hope for new antimalarial drugs. *Expert Rev Clin Pharmacol* **2**, 469–489 (2009).
12. Ancelin, M. L. *et al.* Potent inhibitors of Plasmodium phospholipid metabolism with a broad spectrum of in vitro antimalarial activities. *Antimicrob Agents Chemother* **47**, 2590–2597 (2003).
13. Wein, S. *et al.* Transport and pharmacodynamics of albitiazolium, an antimalarial drug candidate. *Br J Pharmacol* **166**, 2263–2276 (2012).
14. Wein, S. *et al.* High Accumulation and In Vivo Recycling of the New Antimalarial Albitiazolium Lead to Rapid Parasite Death. *Antimicrob Agents Chemother* **61**, (2017).
15. Wein, S. *et al.* Contribution of the precursors and interplay of the pathways in the phospholipid metabolism of the malaria parasite. *J Lipid Res* **59**, 1461–1471 (2018).
16. Huang, H. K. H. *et al.* The membrane-binding domain of an amphitropic enzyme suppresses catalysis by contact with an amphipathic helix flanking its active site. *J Mol Biol* **425**, 1546–1564 (2013).
17. Taneva, S. G. *et al.* Interdomain communication in the phosphatidylcholine regulatory enzyme, CCTα, relies on a modular αE helix. *Journal of Biological Chemistry* **294**, 15517–15530 (2019).
18. Johnson, J. E., Xie, M., Singh, L. M. R., Edge, R. & Cornell, R. B. Both acidic and basic amino acids in an amphitropic enzyme, CTP:phosphocholine cytidylyltransferase, dictate its selectivity for anionic membranes. *Journal of Biological Chemistry* **278**, 514–522 (2003).
19. Chong, S. S. Y., Taneva, S. G., Lee, J. M. C. & Cornell, R. B. The curvature sensitivity of a membrane-binding amphipathic helix can be modulated by the charge on a flanking region. *Biochemistry* **53**, 450–461 (2014).

20. Cornell, R. B. Membrane lipid compositional sensing by the inducible amphipathic helix of CCT. *Biochimica et Biophysica Acta - Molecular and Cell Biology of Lipids* vol. 1861 847–861 Preprint at https://doi.org/10.1016/j.bbalip.2015.12.022 (2016).

21. Larvor, M.-P. *et al. Characterization of the lipid-binding domain of the Plasmodium falciparum CTP:phosphocholine cytidylyltransferase through synthetic-peptide studies*. *Biochem. J* vol. 375 (2003).

22. Cornell, R. B. & Ridgway, N. D. CTP:phosphocholine cytidylyltransferase: Function, regulation, and structure of an amphitropic enzyme required for membrane biogenesis. *Progress in Lipid Research* vol. 59 147–171 Preprint at https://doi.org/10.1016/j.plipres.2015.07.001 (2015).

23. Contet, A. *et al.* Plasmodium falciparum CTP:phosphocholine cytidylyltransferase possesses two functional catalytic domains and is inhibited by a CDP-choline analog selected from a virtual screening. *FEBS Lett* **589**, 992–1000 (2015).

24. Esko, J. D. & Raetz, C. R. Autoradiographic detection of animal cell membrane mutants altered in phosphatidylcholine synthesis. *Proc Natl Acad Sci U S A* **77**, 5192–5196 (1980).

25. Esko, J. D., Wermuth, M. M. & Raetz, C. R. Thermolabile CDP-choline synthetase in an animal cell mutant defective in lecithin formation. *Journal of Biological Chemistry* **256**, 7388–7393 (1981).

26. Esko, J. D., Nishijima, M. & Raetz, C. R. Animal cells dependent on exogenous phosphatidylcholine for membrane biogenesis. *Proceedings of the National Academy of Sciences* **79**, 1698–1702 (1982).

27. Marton, L. *et al.* Heterologous expression of CTP: Phosphocholine cytidylyltransferase from Plasmodium falciparum rescues Chinese Hamster Ovary cells deficient in the Kennedy phosphatidylcholine biosynthesis pathway. *Sci Rep* **8**, (2018).

28. Cui, Z. *et al.* A genetic defect in phosphatidylcholine biosynthesis triggers apoptosis in Chinese hamster ovary cells. *Journal of Biological Chemistry* **271**, 14668–14671 (1996).

29. Hyde, J. Targeting Purine and Pyrimidine Metabolism in Human Apicomplexan Parasites. *Curr Drug Targets* **8**, 31–47 (2006).

30. Belen Cassera, M., Zhang, Y., Z. Hazleton, K. & L. Schramm, V. Purine and Pyrimidine Pathways as Targets in Plasmodium falciparum. *Curr Top Med Chem* **11**, 2103–2115 (2011).

31. Rieckmann, K. H., Yeo, A. E. T. & Edstein, M. D. Activity of PS-15 and its metabolite, WR99210, against Plasmodium falciparum in an in vivo-in vitro model. *Trans R Soc Trop Med Hyg* **90**, 568–571 (1996).

32. Guca, E. *et al.* Structural determinants of the catalytic mechanism of Plasmodium CCT, a key enzyme of malaria lipid biosynthesis. *Sci Rep* **8**, (2018).

33. Toenhake, C. G. *et al.* Chromatin Accessibility-Based Characterization of the Gene Regulatory Network Underlying Plasmodium falciparum Blood-Stage Development. *Cell Host Microbe* **23**, 557-569.e9 (2018).

34. Purhonen, J., Banerjee, R., McDonald, A. E., Fellman, V. & Kallijärvi, J. A sensitive assay for dNTPs based on long synthetic oligonucleotides, EvaGreen dye and inhibitor-resistant high-fidelity DNA polymerase. *Nucleic Acids Res* **48**, e87–e87 (2020).

35. Nagy, G. N. *et al.* Evolutionary and mechanistic insights into substrate and product accommodation of CTP:phosphocholine cytidylyltransferase from Plasmodium falciparum. in *FEBS Journal* vol. 280 3132–3148 (2013).

36. Murithi, J. M. *et al.* Combining Stage Specificity and Metabolomic Profiling to Advance Antimalarial Drug Discovery. *Cell Chem Biol* **27**, 158-171.e3 (2020).

37. Molnár, P., Marton, L., Izrael, R., Pálinkás, H. L. & Vértessy, B. G. Uracil moieties in Plasmodium falciparum genomic DNA. *FEBS Open Bio* **8**, 1763–1772 (2018).